

Series Editor
Jean-Paul Bourrières

Analysis, Modeling and Stability of Fractional Order Differential Systems 2

The Infinite State Approach

Jean-Claude Trigeassou
Nezha Maamri

Color section

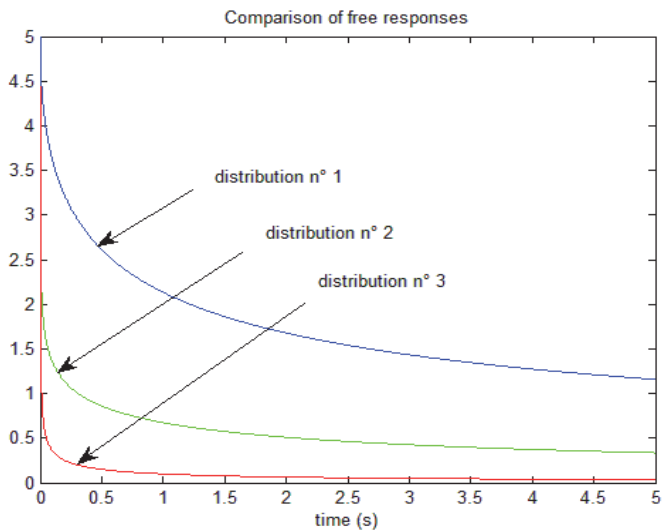


Figure 1.3. Free responses with the same initial value

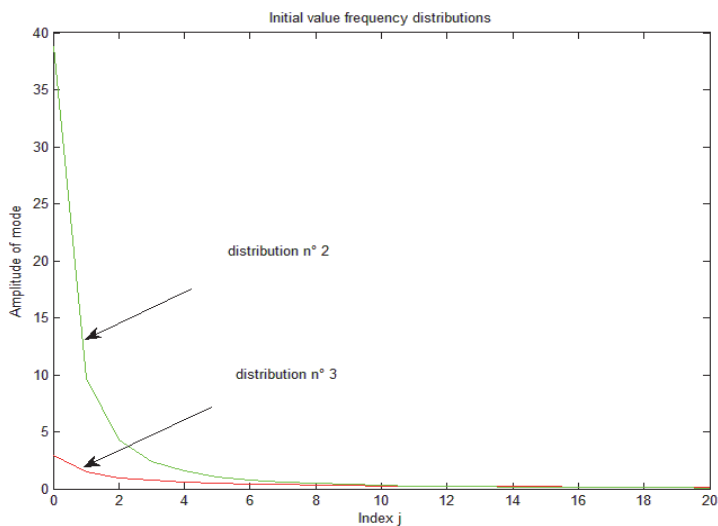


Figure 1.4. Comparison of distributions 2 and 3

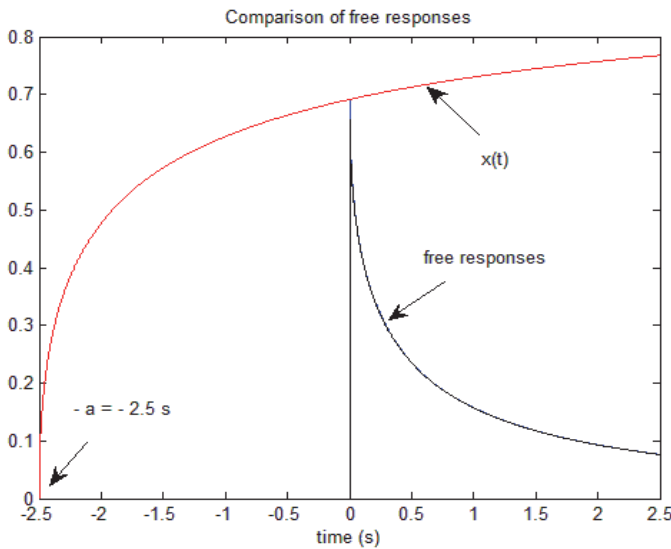


Figure 1.5. Comparison of initialization functions

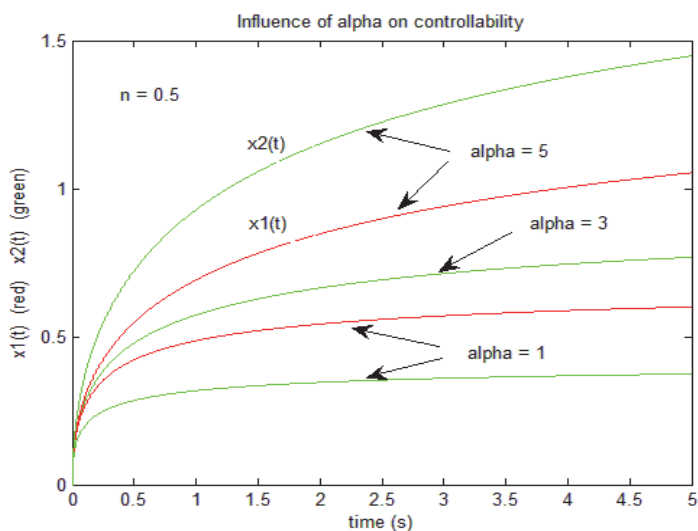


Figure 2.1. Pseudo-controllability of the commensurate order case

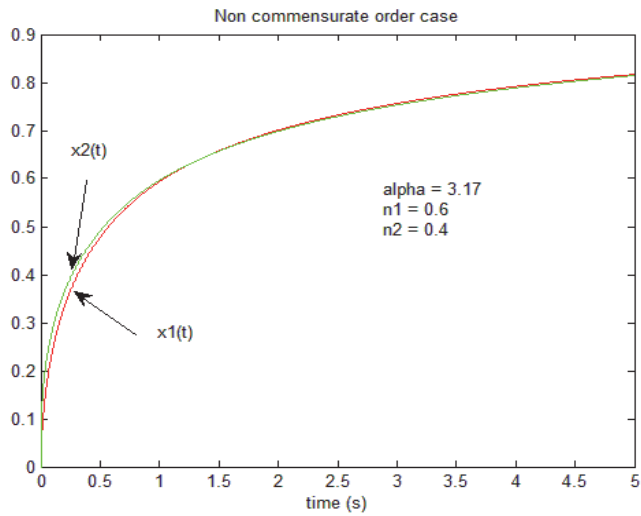


Figure 2.2. Pseudo-controllability of the non-commensurate order case

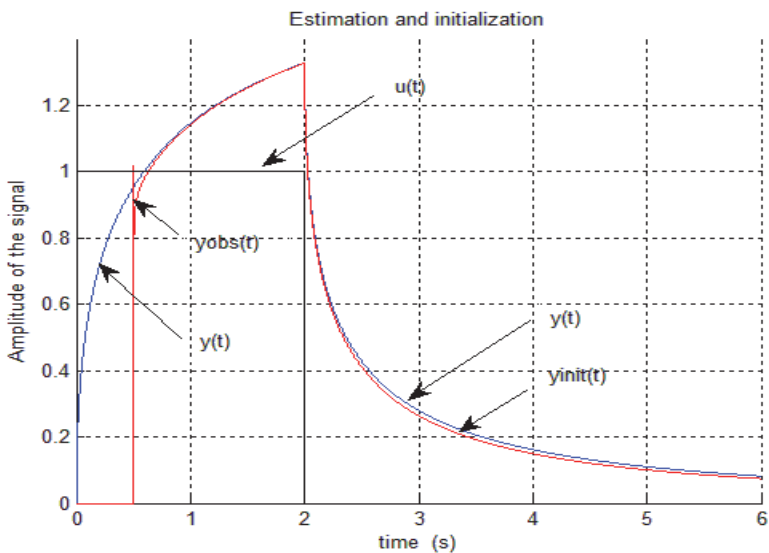


Figure 3.1. Input $u(t)$ and outputs $y(t)$, $\hat{y}(t)$ and $y_{init}(t)$

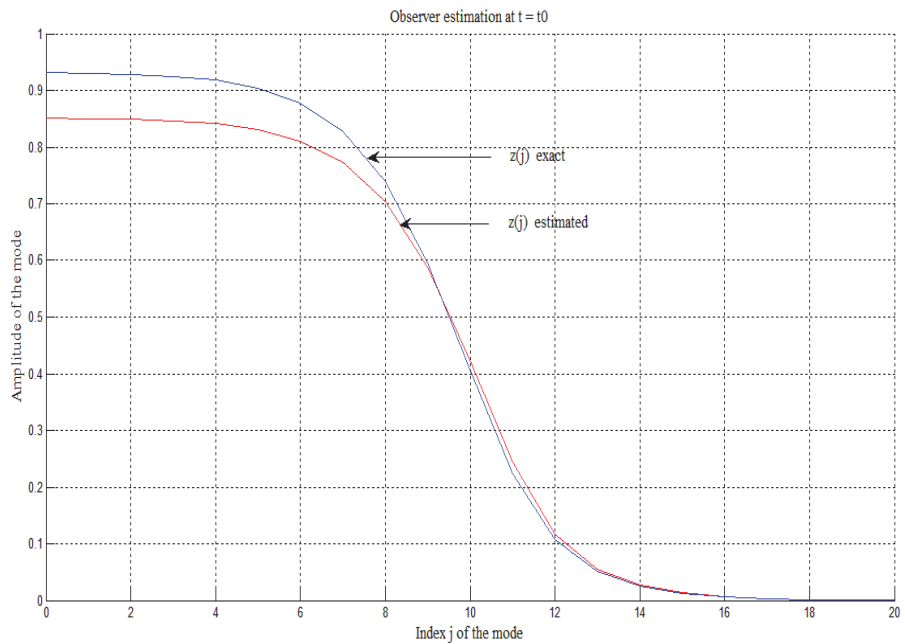


Figure 3.2. Comparison between modes $z_j(t_0)$ and $\hat{z}_j(t_0)$ for $j = 0, 1, 2, \dots, 20$

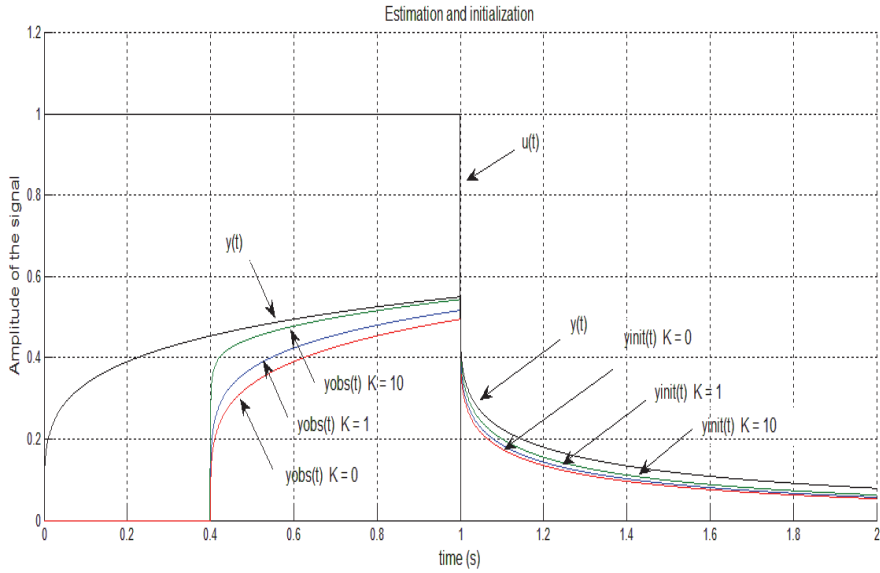


Figure 3.3. $u(t)$, $y(t)$, $\hat{y}(t)$ and $y_{init}(t)$

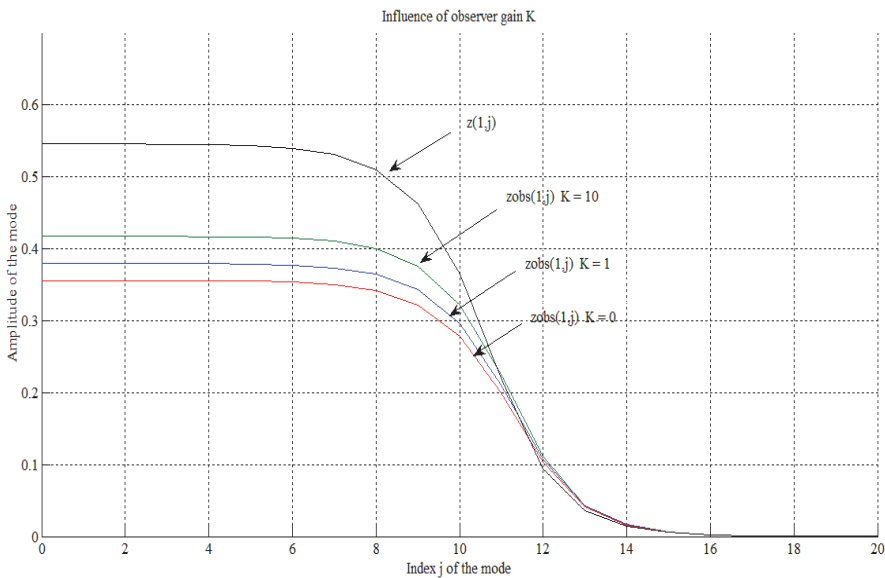


Figure 3.4. Comparison between modes $z_{1,j}(t_0)$ and $\hat{z}_{1,j}(t_0)$ for $j = 0, 1, 2, \dots, 20$

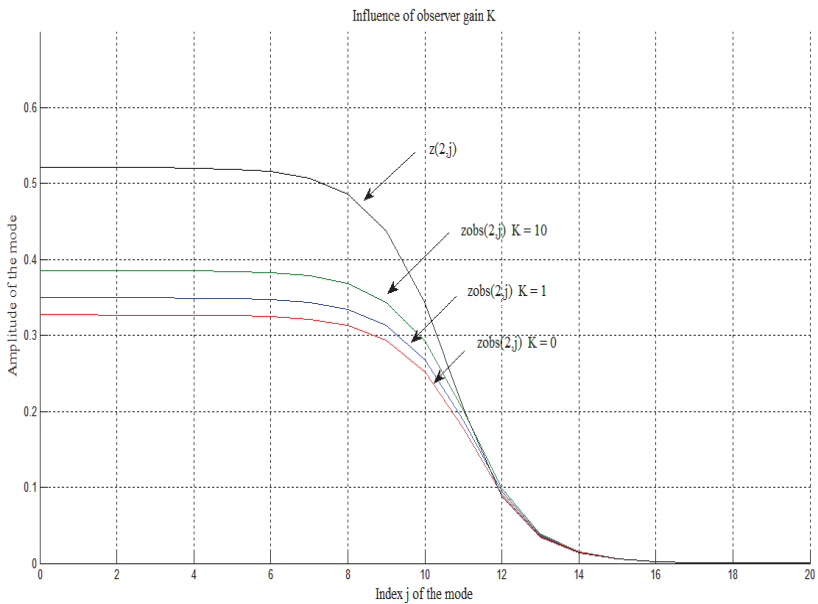


Figure 3.5. Comparison between modes $z_{2,j}(t_0)$ and $\hat{z}_{2,j}(t_0)$ for $j = 0, 1, 2, \dots, 20$

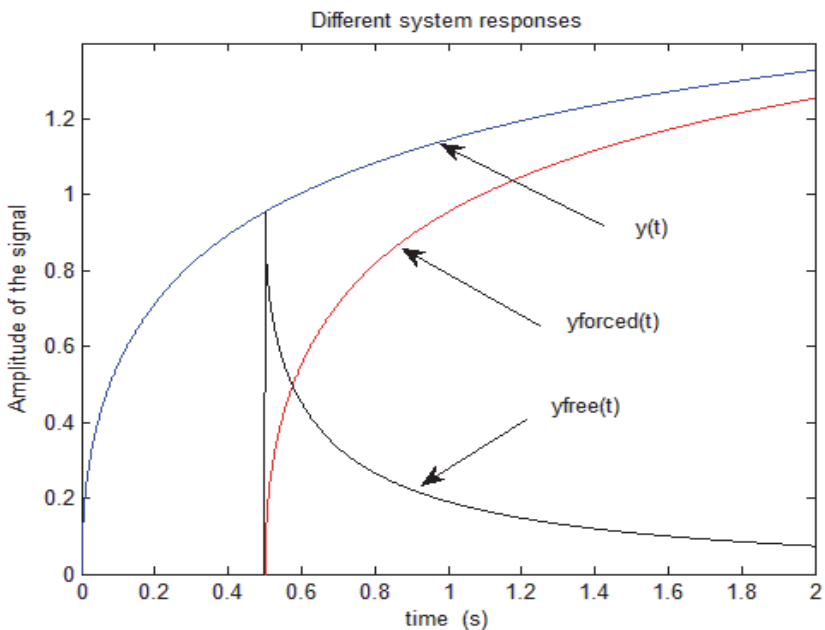


Figure 3.6. The different responses of the system on $[0, t_0]$

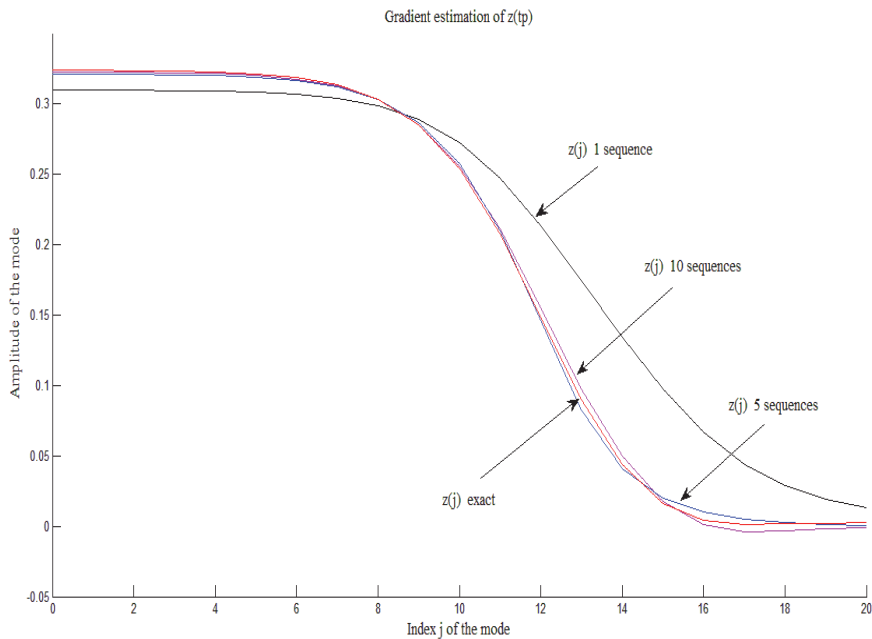


Figure 3.7. Gradient technique estimation of modes $\hat{z}_j(t_p)$ for different sequences

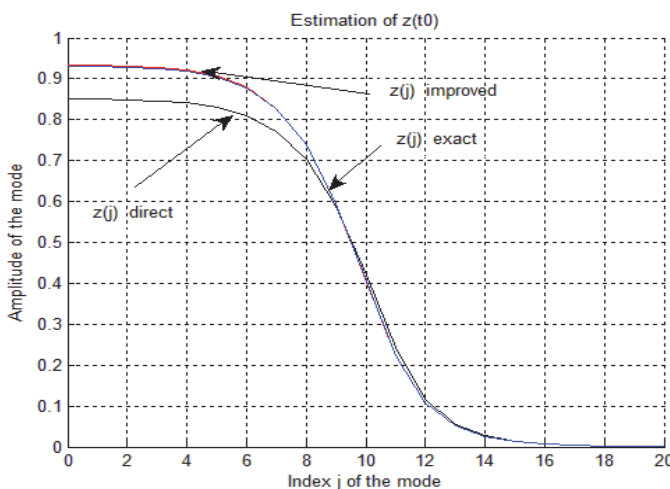


Figure 3.8. Direct and improved estimation $\hat{z}_j(t_0)$ for $j = 0, 1, 2, \dots, 20$

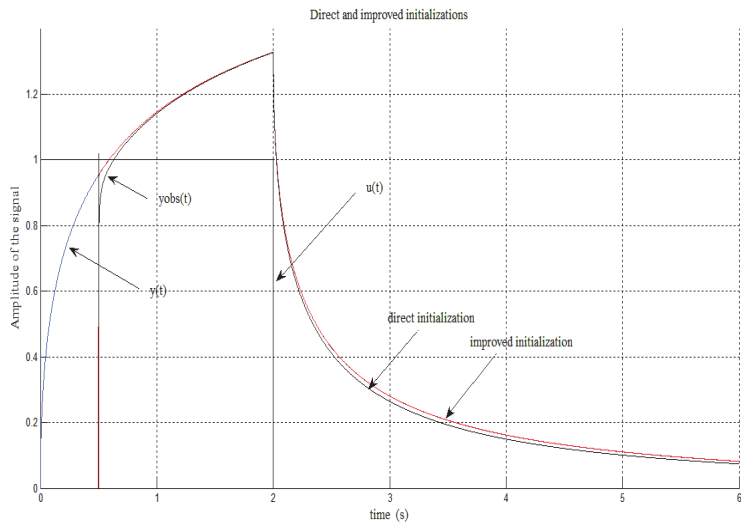


Figure 3.9. $u(t)$, $\hat{y}(t)$ (direct), $\hat{y}(t)$ (improved) and $y_{init}(t)$

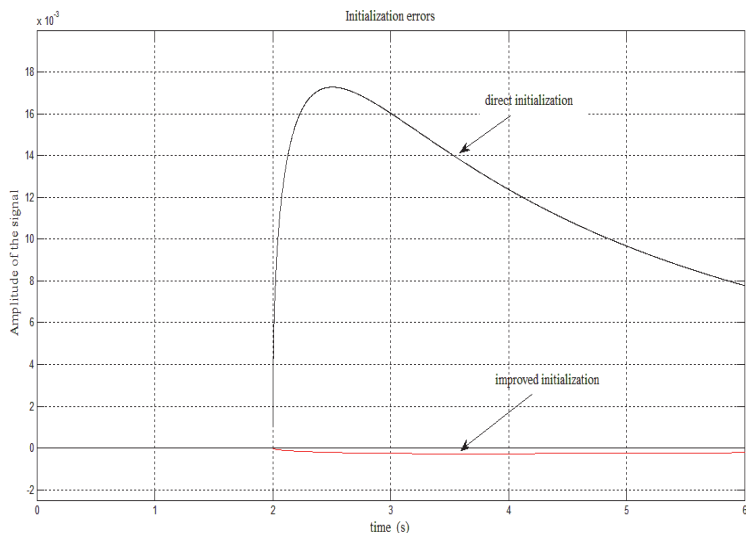


Figure 3.10. Comparison of initialization errors

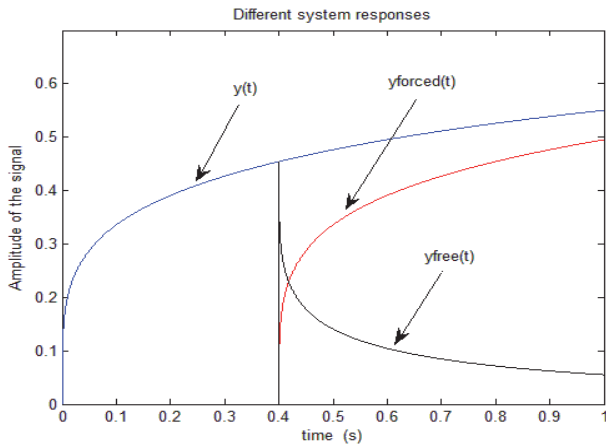


Figure 3.11. The different responses of the system on $[0, t_0]$

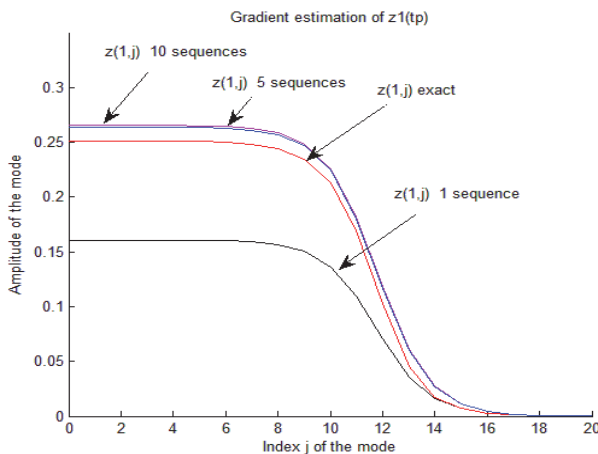


Figure 3.12. Gradient estimation of the modes $\hat{z}_{1,j}(t_p)$ for different sequences

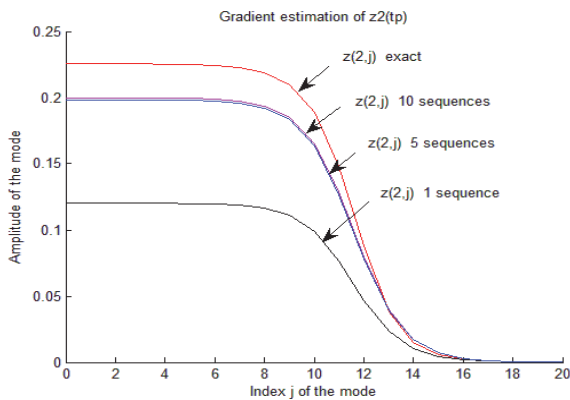


Figure 3.13. Gradient estimation of the modes $\hat{z}_{2,j}(t_p)$ for different sequences

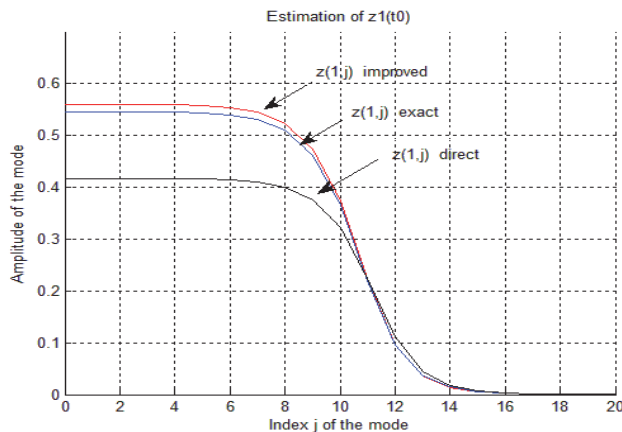


Figure 3.14. Direct and improved estimations $\hat{z}_{1,j}(t_0)$

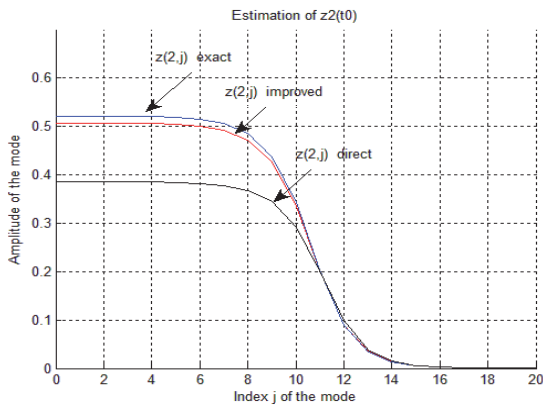


Figure 3.15. Direct and improved estimations $\hat{z}_{2,j}(t_0)$

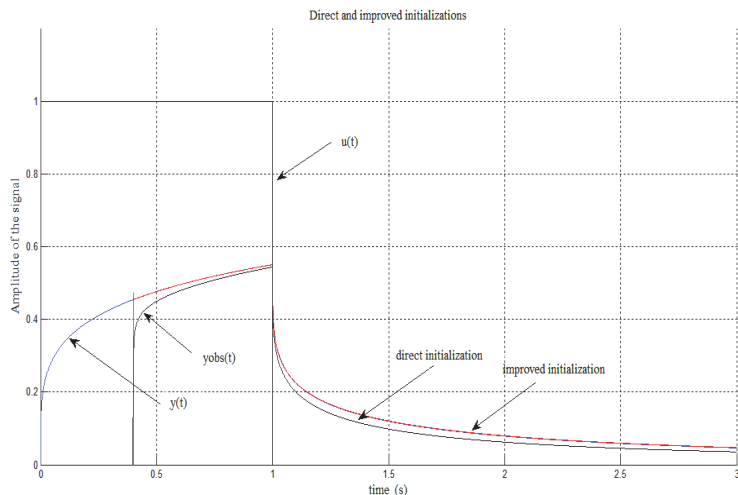


Figure 3.16. $u(t)$, $y(t)$, $\hat{y}(t)$ (direct) and $\hat{y}(t)$ (improved)

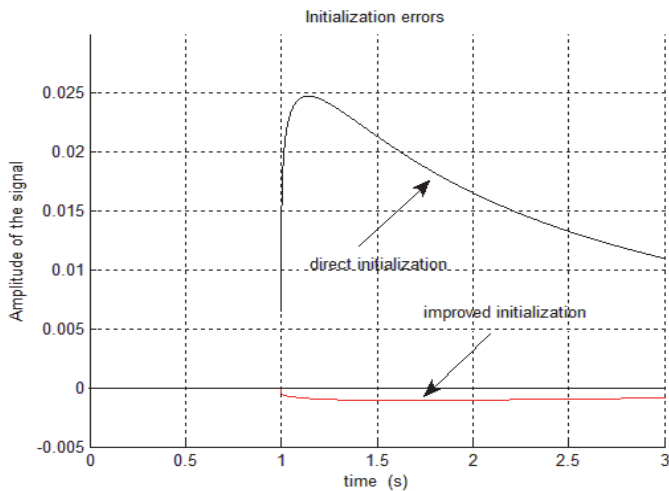


Figure 3.17. Comparison of initialization errors

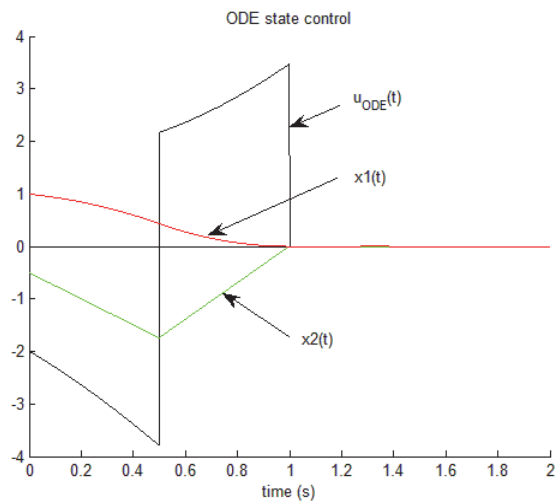


Figure 4.1. ODE state control

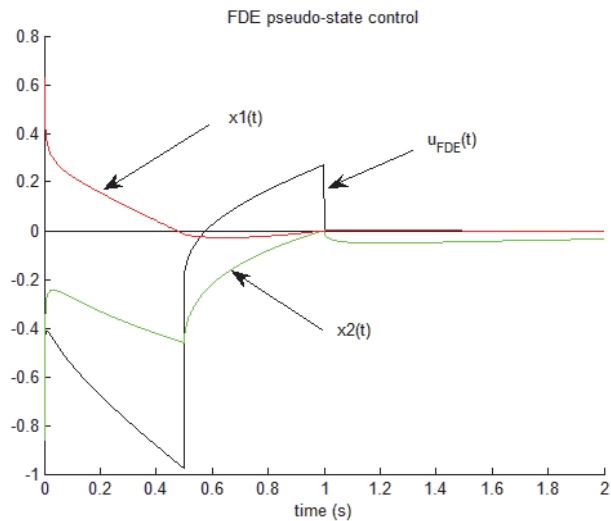


Figure 4.2. FDE pseudo-state control

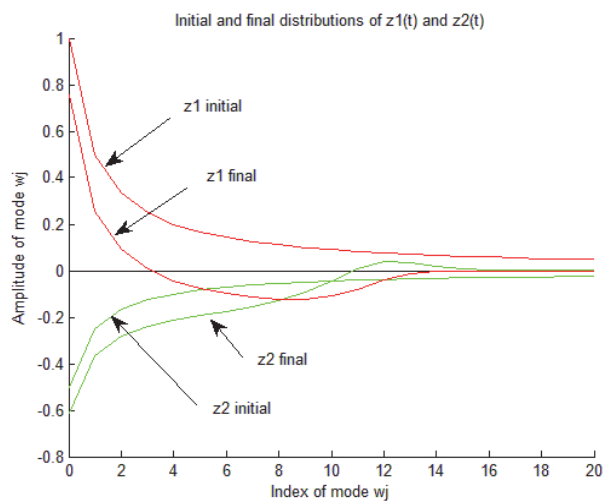


Figure 4.3. Distributions of FDE internal states

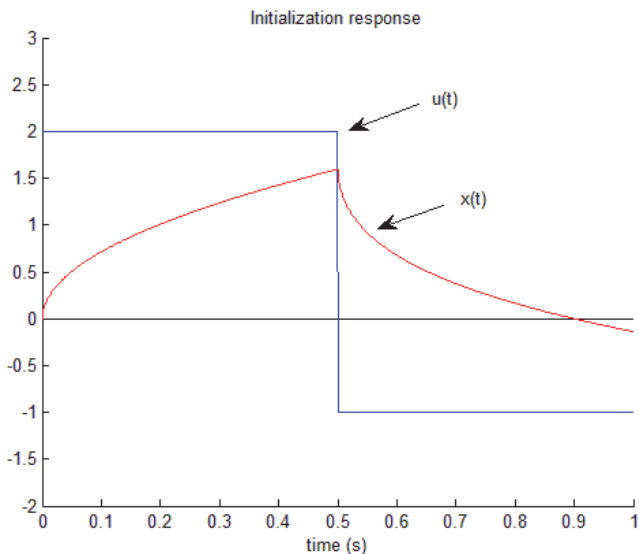


Figure 4.4. Initialization procedure

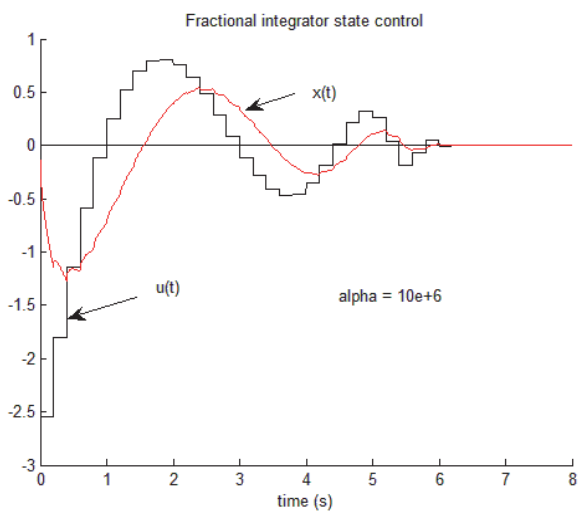


Figure 4.5. Fractional integrator state control

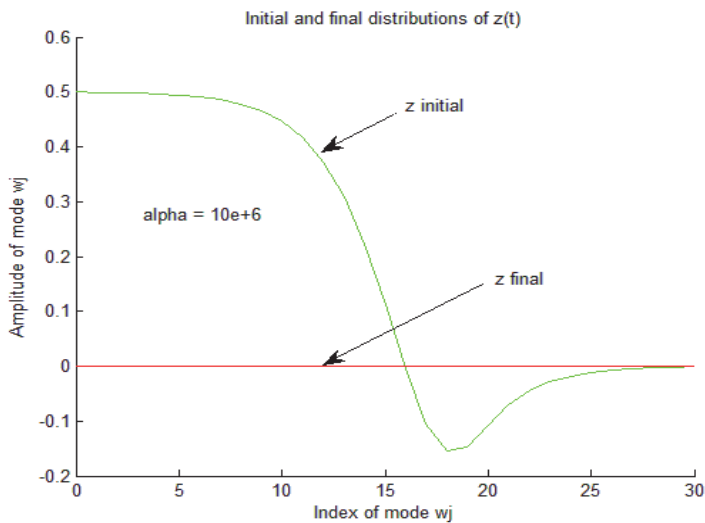


Figure 4.6. Initial and final distributions of the internal state

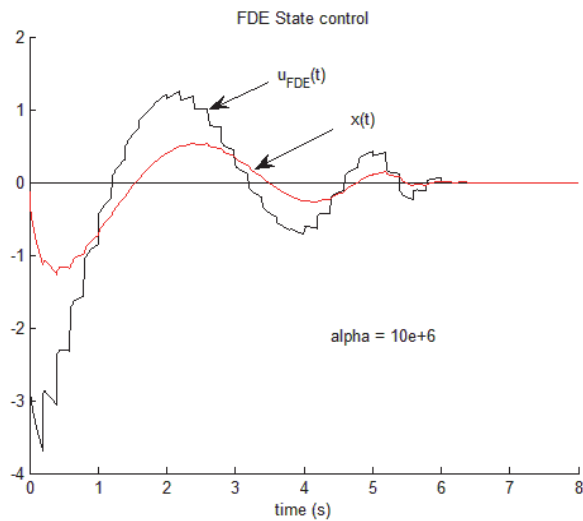


Figure 4.8. FDE state control

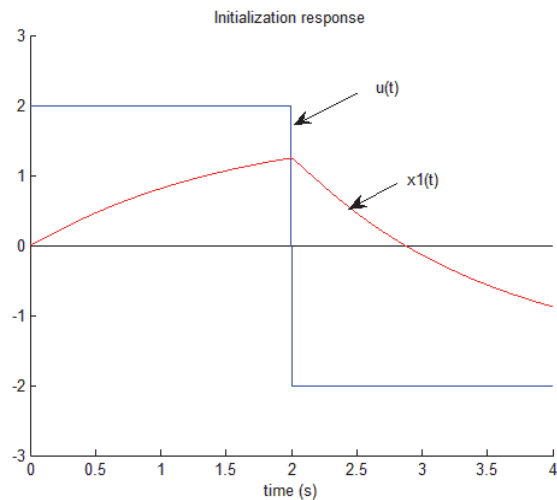


Figure 4.10. Initialization procedure

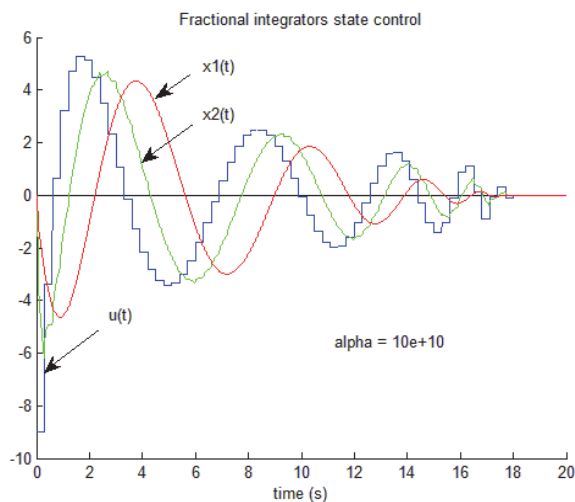


Figure 4.11. State control of two fractional integrators in series

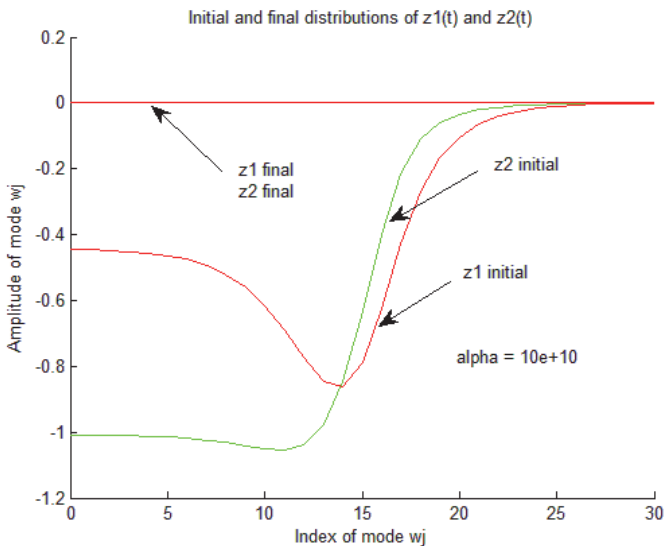


Figure 4.12. Distribution of initial and final internal states

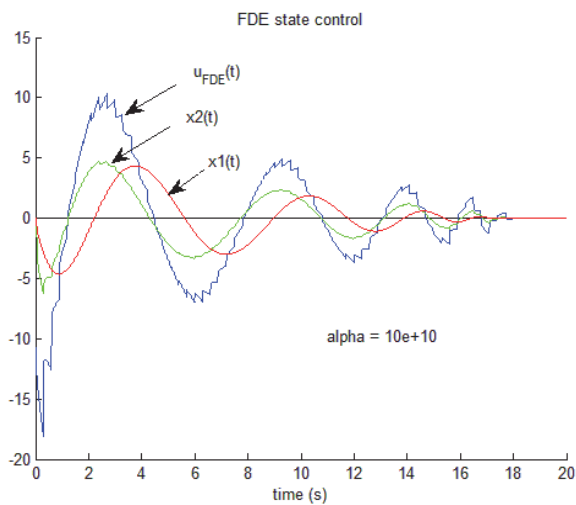


Figure 4.13. Two-derivative FDE state control

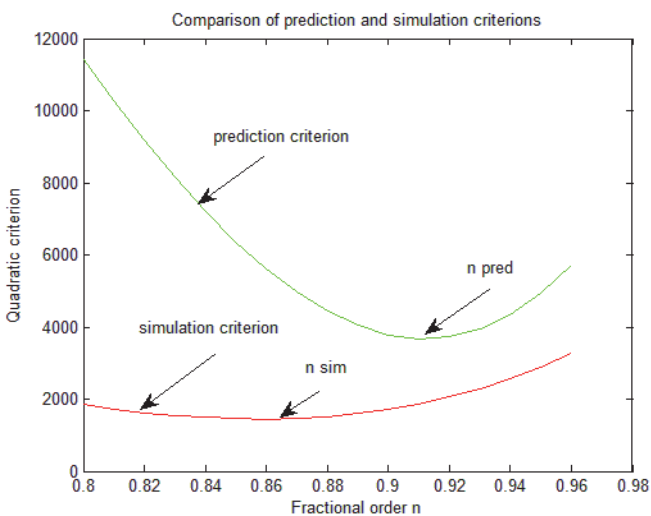


Figure 5.1. Prediction and simulation quadratic criteria

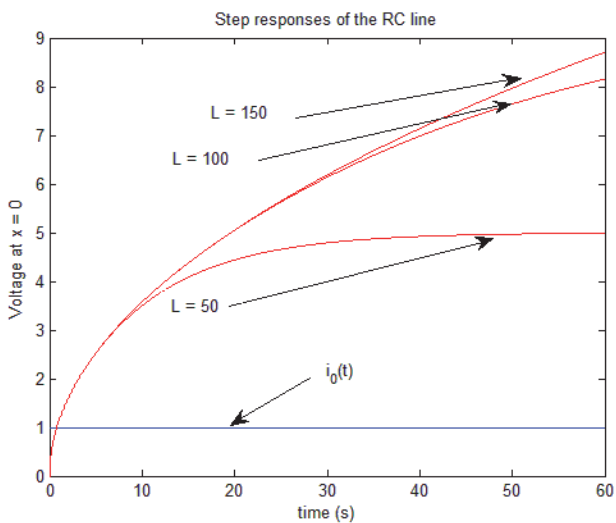


Figure 5.6. Step responses of the RC line

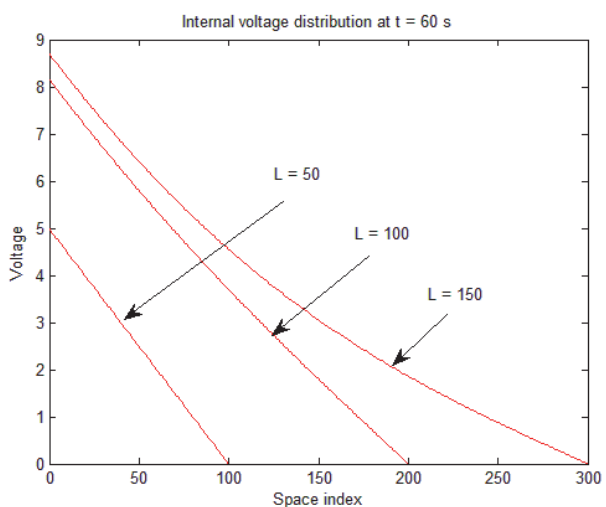


Figure 5.7. Internal voltage distributions

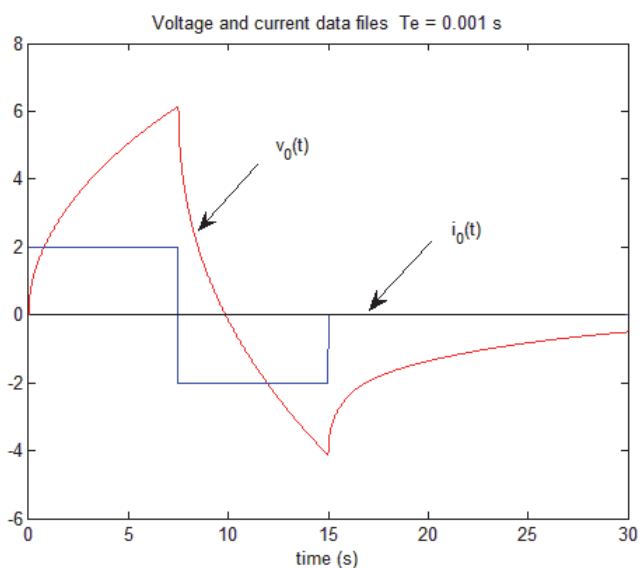


Figure 5.8. Data file: $T_e = 10^{-03}$ s

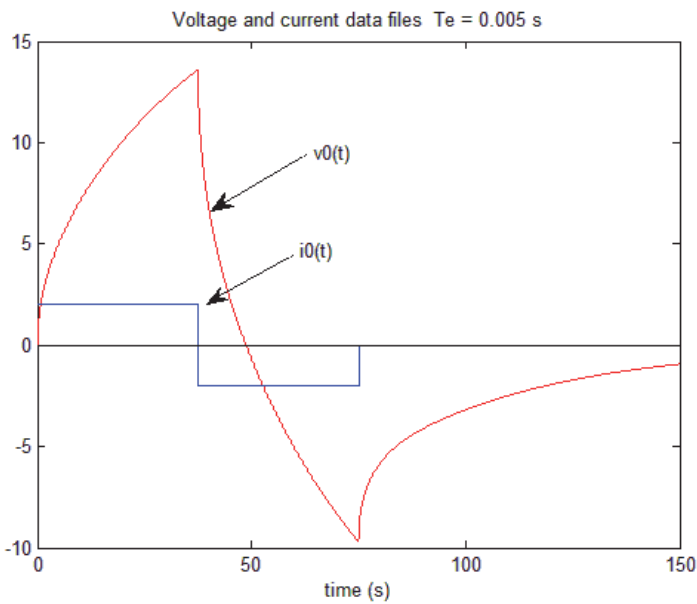


Figure 5.9. Data file: $T_e = 5E^{-03}s$

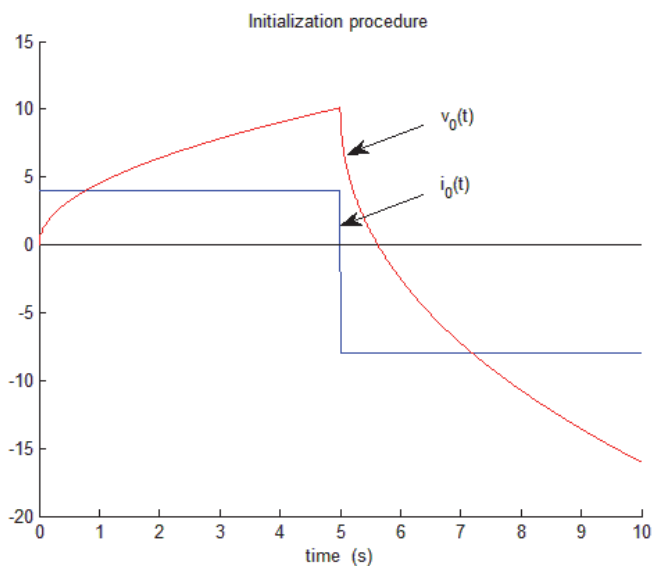


Figure 5.10. Initialization procedure

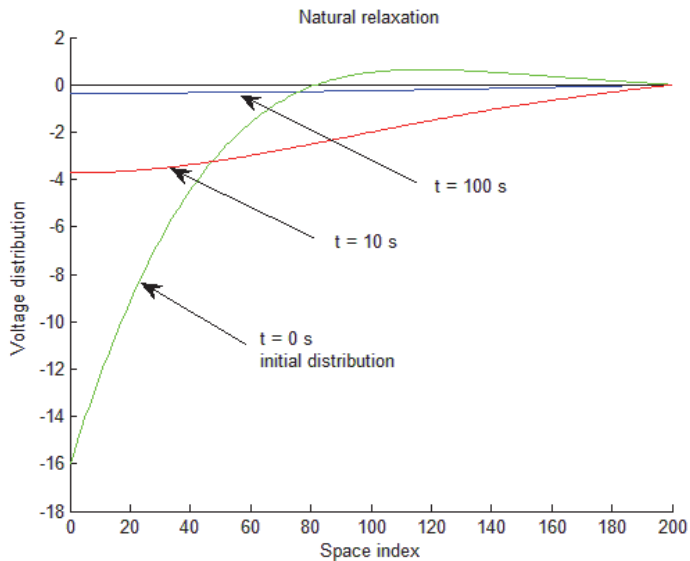


Figure 5.11. Natural relaxation of the RC line

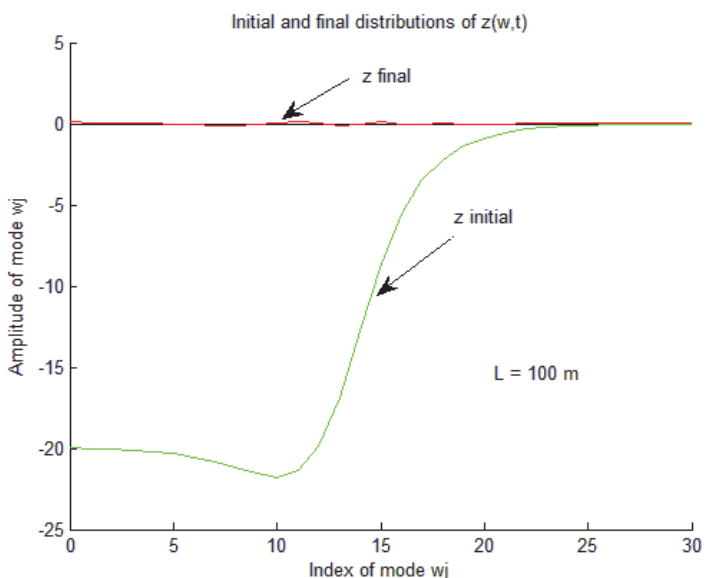


Figure 5.12. Initial and final distribution of the distributed state

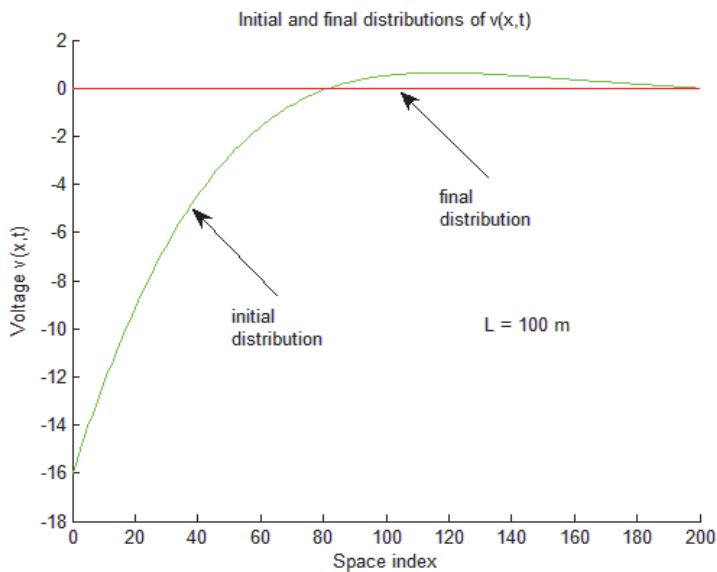


Figure 5.13. Initial and final distribution of the space variable

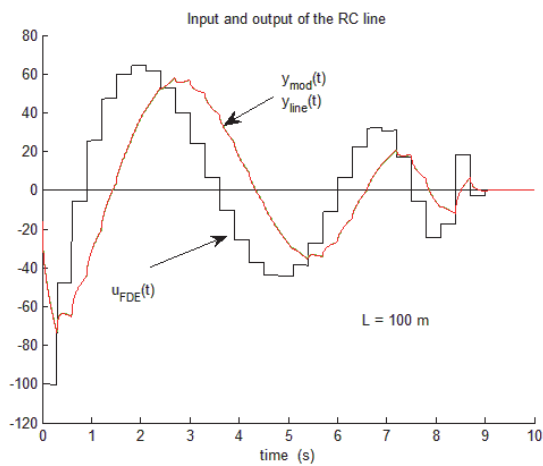


Figure 5.14. Excitation and response of the RC line

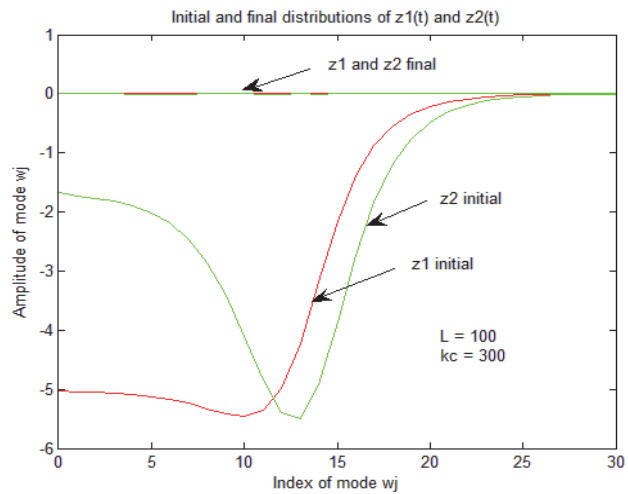


Figure 5.15. Initial and final distribution of the distributed states

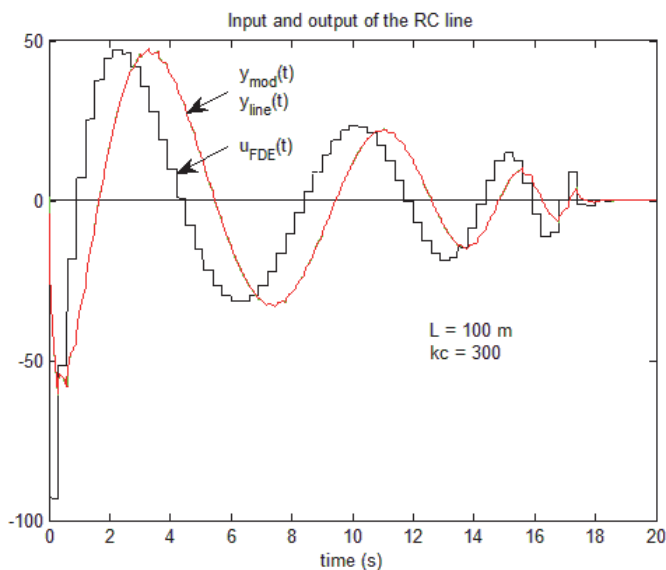


Figure 5.16. Excitation and response of the RC line

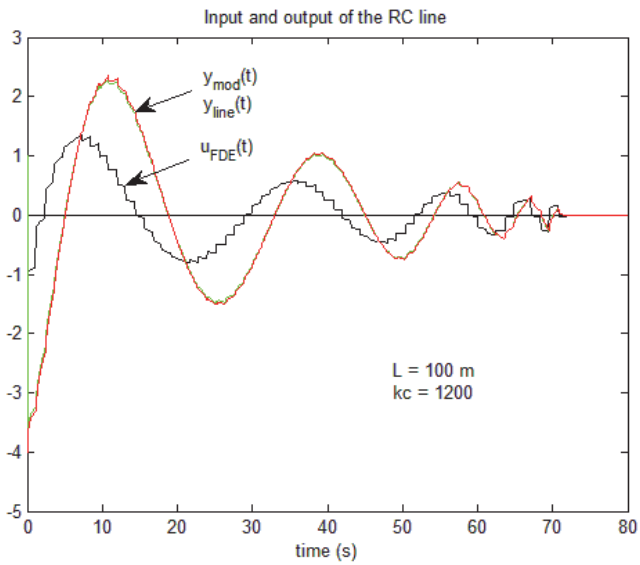


Figure 5.17. Excitation and response of the RC line

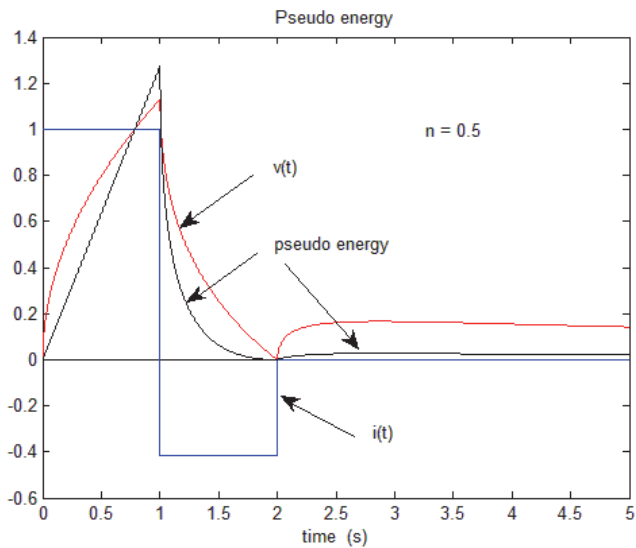


Figure 7.4. Pseudo-energy of the fractional integrator

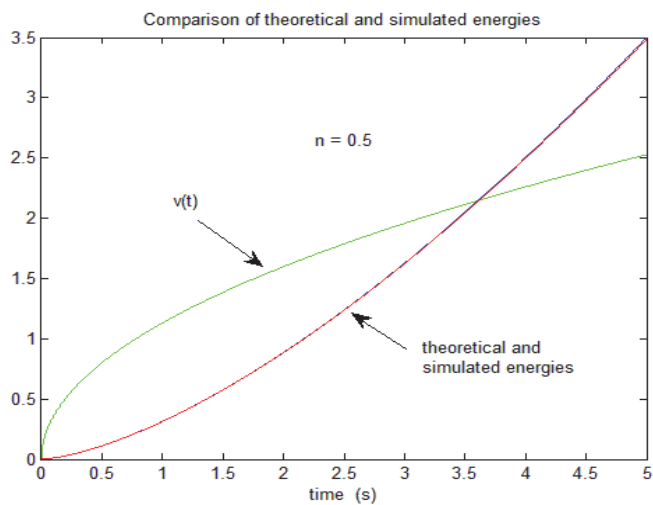


Figure 7.10. Theoretical and simulated energies

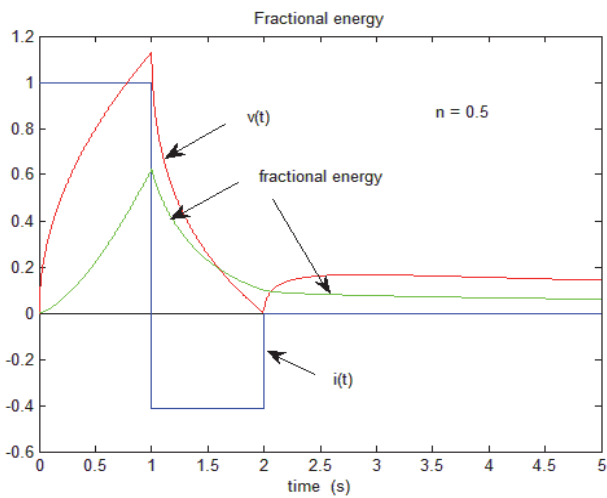


Figure 7.11. Fractional energy

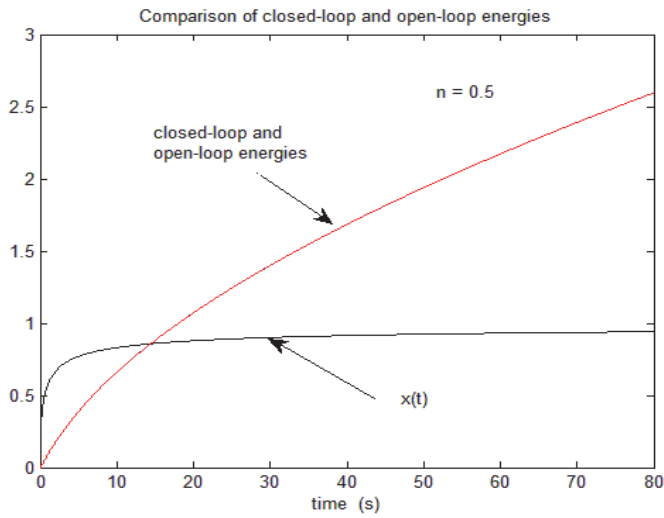


Figure 7.13. Closed-loop and open-loop energies

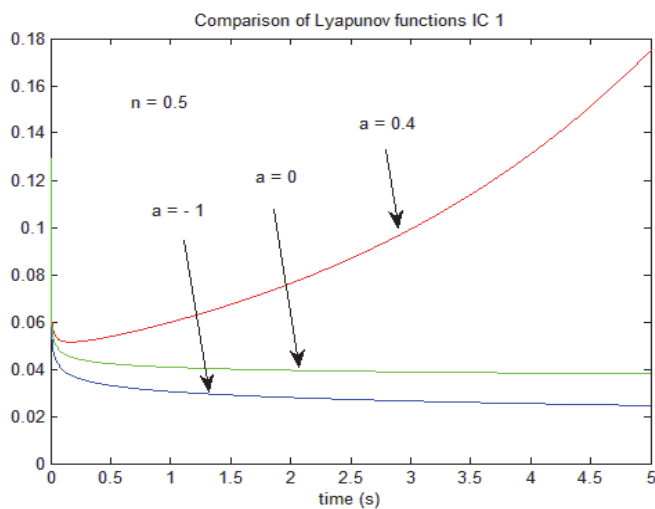


Figure 8.1. Comparison of Lyapunov functions with IC₁

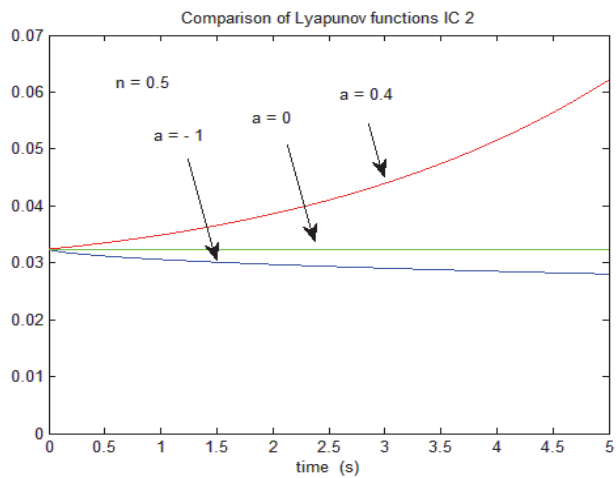


Figure 8.2. Comparison of Lyapunov functions with IC₂

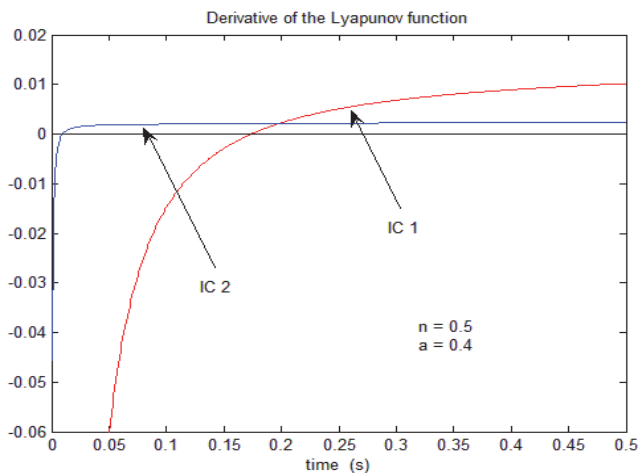


Figure 8.3. Derivative of the Lyapunov function with IC₁ and IC₂

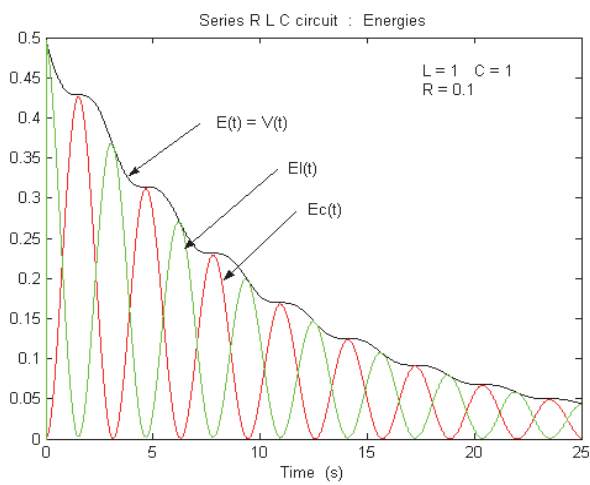


Figure 9.6. Energies of the series RLC circuit

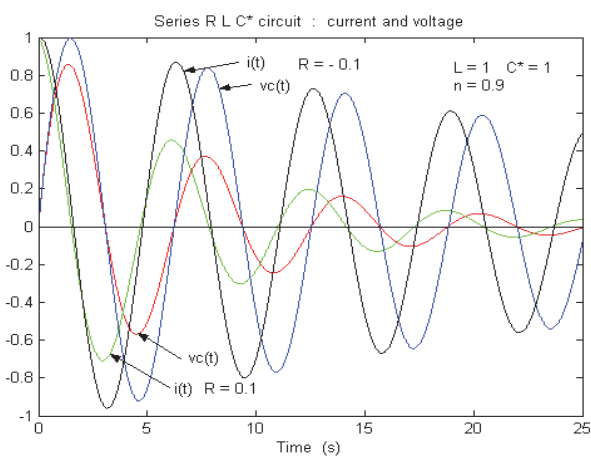


Figure 9.7. Current and voltage of the RLC* circuit

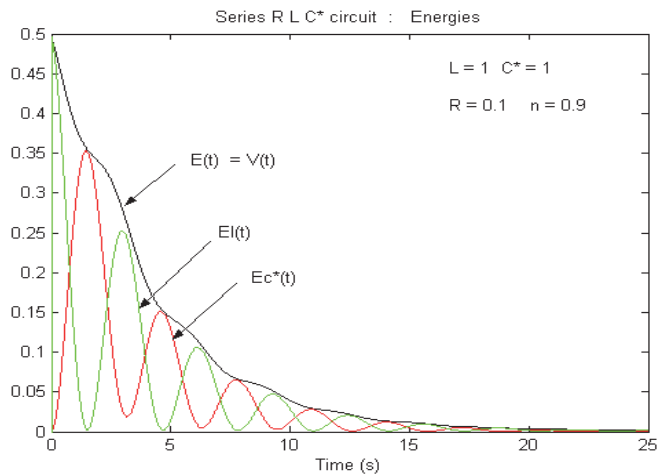


Figure 9.8. Energy of the RLC^* circuit, $R = 0.1$

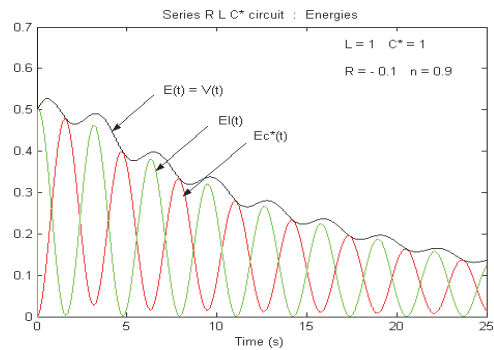


Figure 9.9. Energy of the RLC^* circuit, $R = -0.1$

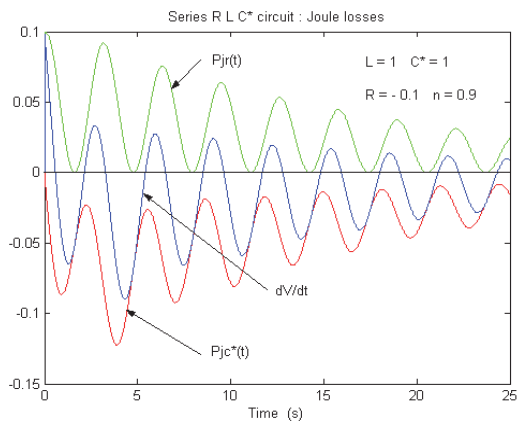


Figure 9.10. Derivative of the Lyapunov function

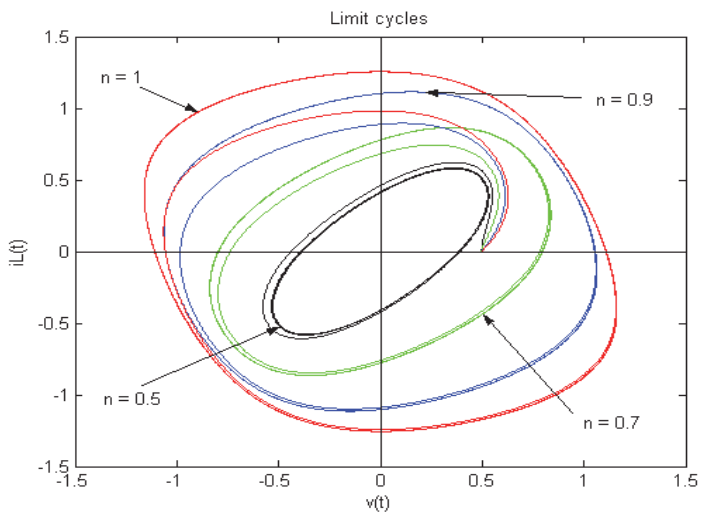


Figure 10.5. Influence of the fractional order n

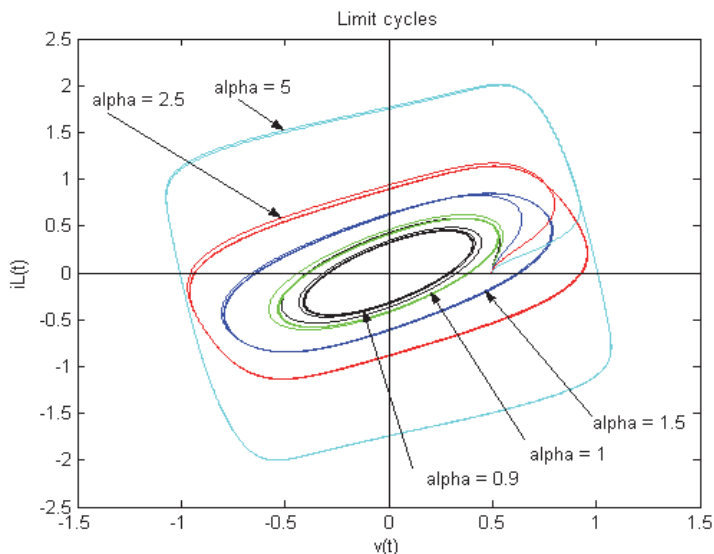


Figure 10.6. Influence of the parameter α

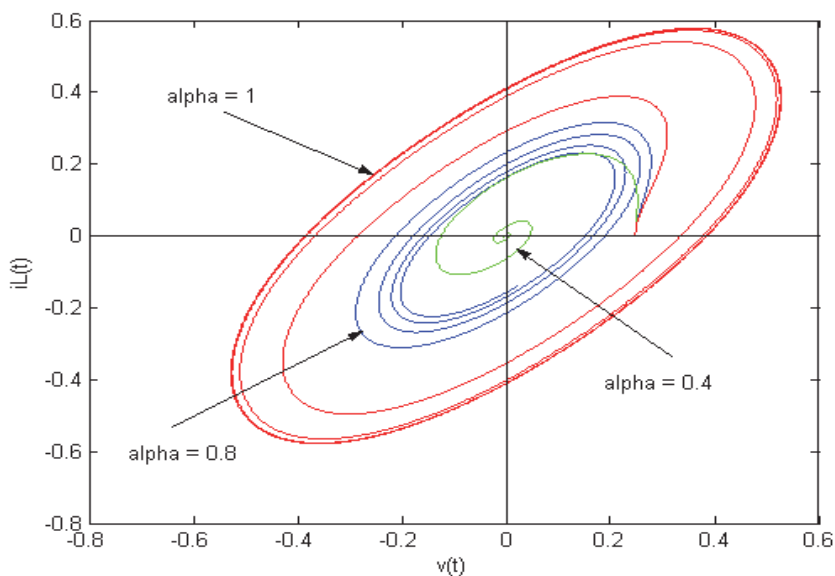


Figure 10.7. Stability of the Van der Pol system

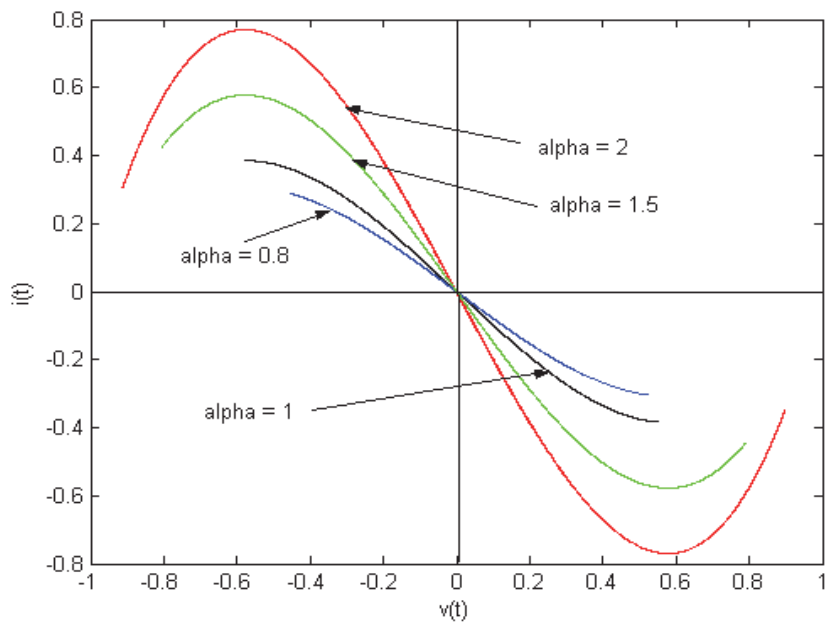


Figure 10.8. Nonlinear characteristic $i=f(v)$